Crop Type Identification and Classification by Reflectance Using Satellite Images

Maheswarappa B., Dr. H. R. Sudarshan Reddy

[1]*Professor, Department of Electronics and Communication, S T J I T, Ranebennur, Karnataka, India*
[2]*Professor, Department of Electrical & Electronics Engineering, University B. D. T. College of Engineering, Davangere. Karnataka, India*

Abstract: **Identification of crop types, accurately and timing is the one the application of remote sensing, It helps the people to control the variations in the prices of the food grains. Remote sensing methods to identify crop types rely on remotely sensed images of high temporal frequency in order to utilize phenological changes in crop reflectance characteristics. Image sets have generally low spatial resolution. This makes difficult to classify crop types were field sizes are smaller than the resolution of imaging sensor. Here, we develop a method for combining high resolution data with images with low spatial resolution but with high time frequency to achieve a superior classification of crop types.**

***Key words*— Crops, NDVI, agriculture, classification algorithms, image processing, pattern recognition, vegetation mapping, remote sensing.**

I. INTRODUCTION

Paddy, maize and sugarcane are the most cultivated crops in the davanagere district. In particular, remotely sensed agricultural monitoring has received a lot of attention due to the strong impact on food security. Early production estimation can be very important for farmers economic planning, agronomic field management and yield price. The Indian economy is majorly dependent on agriculture as the countries 40 percent income is by means of agriculture[1] i.e. gross national product(GNP) and also provides occupation and livelihood for 70 percent of population, hence agriculture is called backbone of our country. The availability of accurate and timely data on agricultural production would not only help the planners in formulating development programmed in rural areas but also enable them to take appropriate decisions on policies relating to import/export of these commodities well in advance [2]. The crop manufacture approximations remain acquired by captivating creation of crop acres besides the equivalent crop harvest. The harvest reviews remain impartially widespread by plot crop data composed beneath a compound sampling plan that is grounded on a stratified multistage arbitrary sampling enterprise [1]. With the introduction of remote sensing technology around 1970's the potential for improvement in agricultural field over the world has increased statistically. The satellite and space research and spectral sensing of agricultural fields provides useful statistics that are mainly used for improving the harvest of crops like wheat, paddy, sugarcane and groundnuts [4].

The temporal dimension that has been most useful for identifying major crop types [3], [4],[7]. This is because, at any point during the growing season, crops are at different stages of maturity, manifested as differential spectral response in remotely sensed images to build a crop-specific temporal record, different stages of maturity, manifested as differential spectral response in remotely sensed images to build a crop-specific temporal record. However, this spatial detail comes at the cost of reduced temporal availability. Due to predetermined acquisition strategies and obstructions by clouds, only a few high-resolution images are usually available during critical growing periods.

Even though remote sensing – based crop type classification are difficult for a number of reasons. First, locations with a smaller fields [6], it required high-resolution observations. Second, field containing mixtures of crops and non crop surfaces, hence the classification accuracy becomes low. For improve the accuracy of a crop type classification we propose a technique that combination of ideal crop curves of simultaneously incorporates both high- and low-resolution images.

II. METHODOLOGY

A. Problem Formulation.

Due to fields containing mixtures of different crops and non-crop surfaces existing high-resolution image data are not enough to resolve individual fields but are either acquired during that part of the growing season when the crops of interest are least distinguishable or acquired only once, but from the information high-resolution sensor acquired only a few times during the growing season. But with low-resolution image data that are frequently available in order to better distinguish the crops of interest?

Ideal reflectance Crop Curves*:* The first step is to generate ideal reflectance crop curves. These curves contain spectral idealized reflectance values of a crop which varies over the

course of the year as crop growth in its growth cycle. We assumed that for every spectral band of the tested sensors for the crop of interest that ideal crop reflectance curves are available.

For a given a set of images containing high- and low-resolution pixel data, the input data may be referred to as follows:

$X^{hi}_{ij}(t)$ - Observed reflectance value for the high-resolution image at pixel *ij* at time t;

$X^{lo}_{ij}(t)$ - Observed reflectance value for the low-resolution image at pixel *ij* at time t*;*

Yij (t) - Predicted crop type at pixel *ij*.

CY ij(*t*) - Ground reference reflectance value for pixel *ij* at time *t* assuming crop type *Y* .

Using a typical least squares method, above can be expressed by

For high resolution image

$$\sum_{(i,j),t}\left|CY_{i,j}(t) - X^{hi}_{i,j}\right|^2 \quad (1).$$

Using a Gaussian distribution to model a sensor PSF

For low resolution images

$$W((I,j),(k,l),\sigma_p^2) = \frac{1}{\sigma_p\sqrt{2\pi}}\, e^{-(k-i)^2+(l-j)^2/(2\sigma^2)} \quad (2).$$

Where, (*i, j*) - Center of the high-resolution pixel,

(*k, l*) - Center of the low-resolution pixel, and *σp* is the standard deviation of the Gaussian PSF.

Note that both (*i, j*) and (*k, l*) are defined in the same coordinate system.

w(i,j)(k,l) – Probability density function evaluated on the points (*i, j*) and (*k, l*) using a predefined variance *σ*2.

Low-resolution image pixel is the weighted sum of the reflectance values for the corresponding high-resolution pixels.

A larger number of pairs of adjacent pixels which are different will lead to a larger penalty.

$$\sum_{(i,j)with\ neighbor\ (p,q)} 1(Y(i,j) \neq Y(p,q) \quad (3).$$

The equation (3) evaluates 1 if $Y_{(i,j)} \neq Y_{(p,q)}$ and 0 if $Y_{(i,j)} = Y_{(p,q)}$.

If there are n possible crop types, each element in the matrix *Y* can be defined as follows:

$$Y_{i,j} = \begin{pmatrix} 1Y_{ij} \\ 2Y_{ij} \\ 3Y_{ij} \\ \dots\ \dots \\ nY_{ij} \end{pmatrix}$$

B. Implementation

We generated 2-D array, each element in a array is a labeled crop type, in the array without bias for any particular crop type is being represented in the map as similar as in the true map. Next, we selected the size of each field was to be more than a high resolution pixel. in each field 1 to 30 pixels are reasonable sizes for particular crop. Fields should be arranged in an asymmetrical pattern of a different size for a more accuracy. The resulting crop landscape was used as a reasonable representation of a real field. Reflectance values that represented in 2-D array of multispectral image, each pixel is examined for a labeled crop type.

For our experiment, these ideal crop curves are extracted from Landsat 8 data in higher resolution images and taking the reading of temporal changes in reflectance values in each band from shortwave to visible portions of the spectrum.
For a image with a low resolution, we chose resolution of pixel to be equal to the high resolution pixels size of 64 with width and height of the low resolution are eight time greater than the height and width of the high resolution pixel.

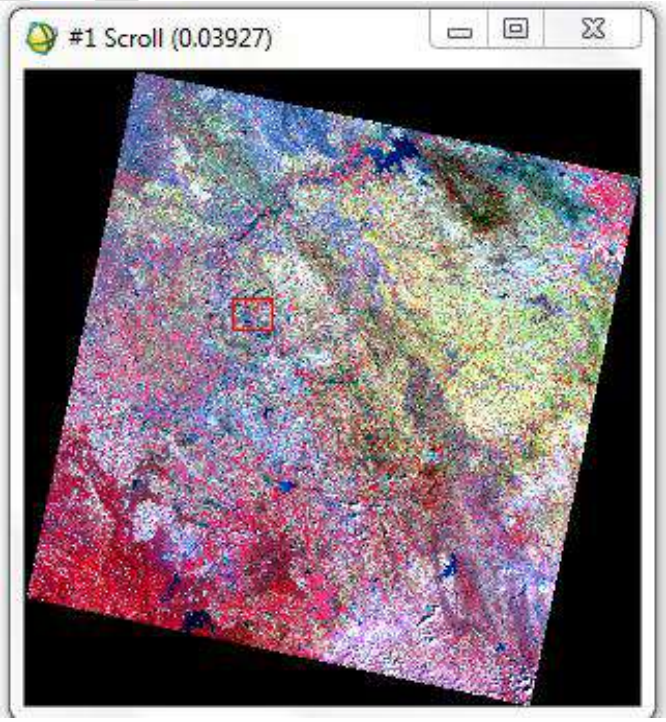

Fig (1) Input Image

Landsat 8 Operational Land Imager (OLI) and Thermal Infrared Sensor (TIRS) Launched February 11, 2013	Bands	Wavelength (micrometers)	Resolution (meters)
	Band 1 - Coastal aerosol	0.43 - 0.45	30
	Band 2 - Blue	0.45 - 0.51	30
	Band 3 - Green	0.53 - 0.59	30
	Band 4 - Red	0.64 - 0.67	30
	Band 5 - Near Infrared (NIR)	0.85 - 0.88	30
	Band 6 - SWIR 1	1.57 - 1.65	30
	Band 7 - SWIR 2	2.11 - 2.29	30
	Band 8 - Panchromatic	0.50 - 0.68	15
	Band 9 - Cirrus	1.36 - 1.38	30
	Band 10 - Thermal Infrared (TIRS) 1	10.60 - 11.19	100 * (30)
	Band 11 - Thermal Infrared (TIRS) 2	11.50 - 12.51	100 * (30)

Table (1) Landsat - 8 Image Specifications

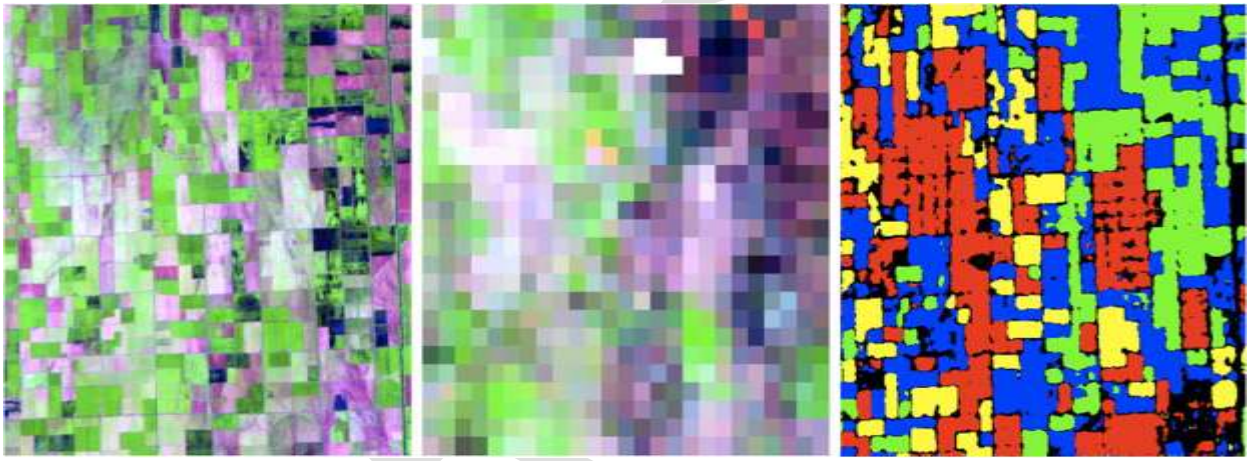

(a) (b) (c)

Fig. (2) . Satellite images. (a) Bands 7–4–2 as (RGB) on July 10, 2015 (b) Bands 7–2–4 s RGB color composite of theLandsat - 8 image. (c) Crop type labels for the real data. Yellow =Maize, Red = Paddy, Green =Arecanuts, Blue = Sugarcane, Black = Unidentified/Background.

Actually we taken (b) Bands 7,2,4 (RGB) is an six-day composite from June 19 through June 25. We selected this image rather than the one closer to July10 because this was the raw image closest in time that was free of clouds.

Image Date	Crop Stages
May 25	Fallow
June 15	Fallow
June 27	Early Maize, Paddy, Sugarcane Planting
Aug 10	Maize Mid-season, Paddy Mid-season, Sugarcane Midseason
Sept 20	Paddy harvest
Oct 7	Maize harvesting
Nov 20	Sugarcane harvesting

Table(2) landsat images used for our study and crop stages that correspond to these dates

To generate the reflectance ideal crop curves, we isolated pixels of each group to each of the crop types in the NASS map by masking. We then aggregated these single crop maps to match the size of MODIS pixels using a cubic convolution re-sampling. Pixels in the aggregated map that had greater than 90% cover for the crop of interest were labeled as pure crop pixels at MODIS scale. We extracted temporal profiles of surface reflectance data across all MODIS bands using only these pure crop pixels and used their average as the ideal crop curves.

III. RESULTS

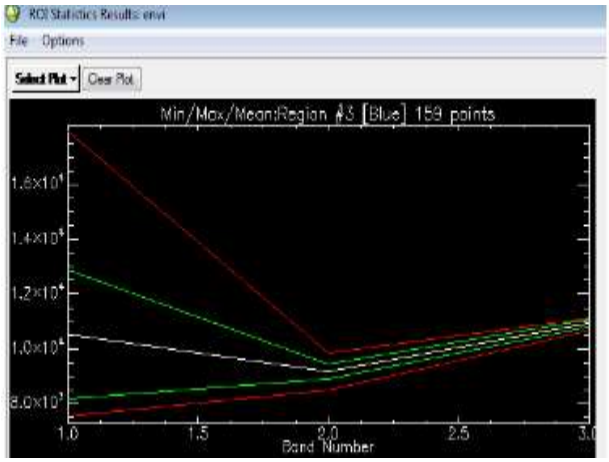

Fig (3) JUNE 15

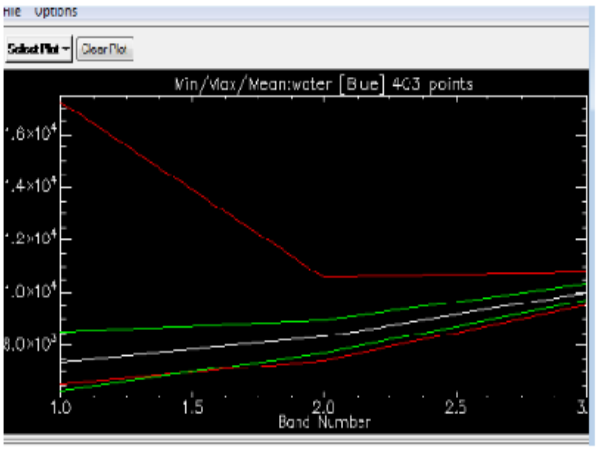

Fig(5) Aug 10

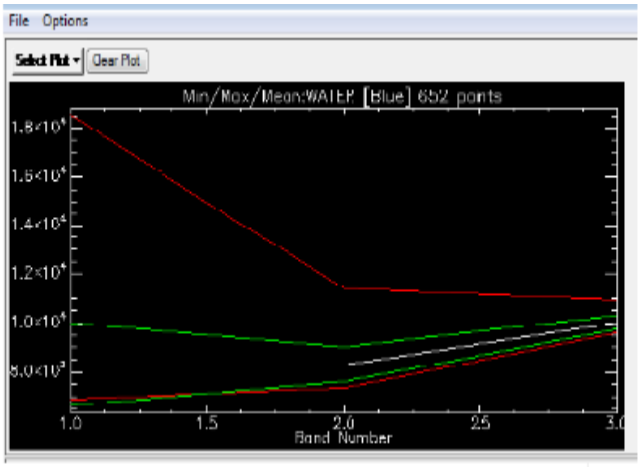

Fig(4) July 27

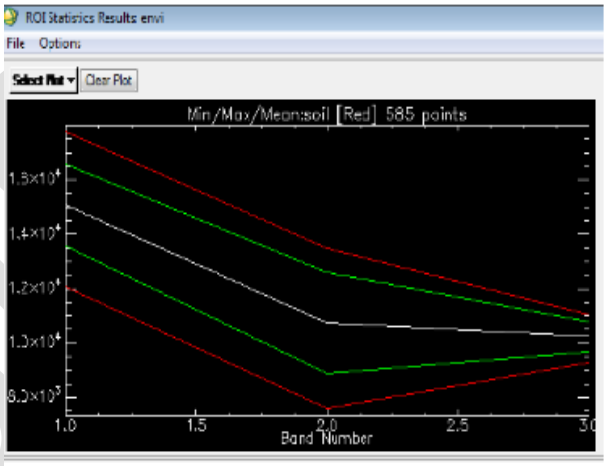

Fig(5) SEPT 20

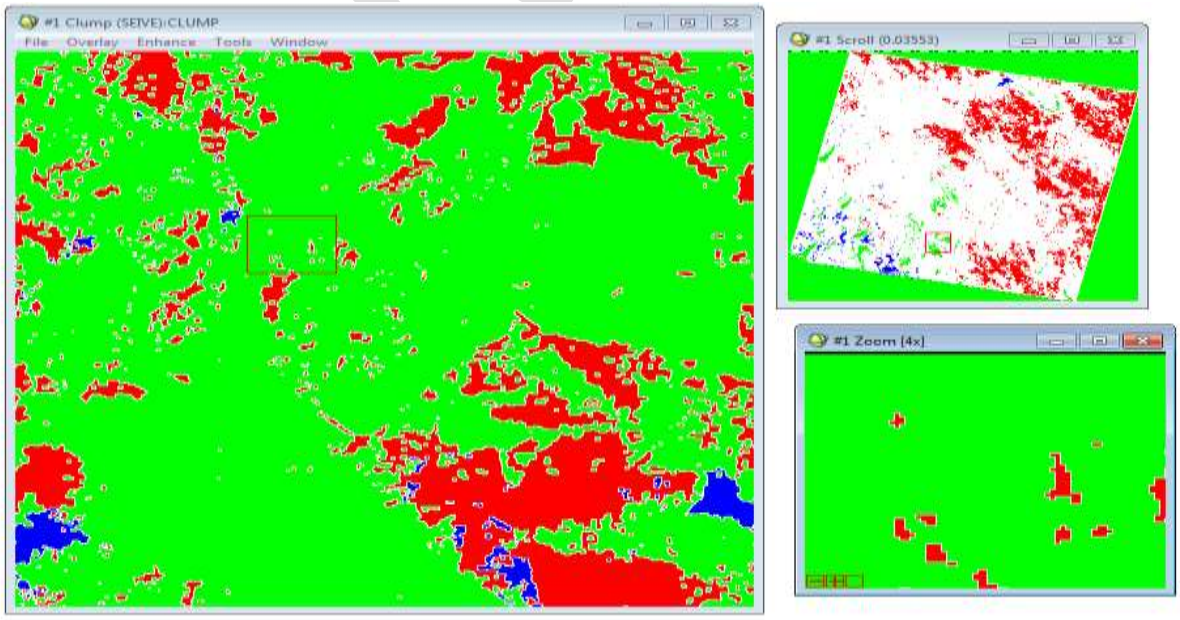

Fig (6) Vector image

Filename: F:\area\march15\clump
Dims: Full Scene (58,607,111 points)

Class Distribution Summary
Region #1 [Red] 696 points: 26,342,564 points (44.948%) (2,370,830.7600 Hectares)
Region #2 [Green] 595 points: 12,934,336 points (22.070%) (1,164,090.2400 Hectares)
Region #3 [Blue] 159 points: 1,734,479 points (2.960%) (156,103.1100 Hectares)
Region #4 [Yellow] 17081452 points: 17,563,104 points (29.968%) (1,580,679.3600 Hectares)

Stats for Class: Region #3 [Blue] 159 points

Basic Stats	Min	Max	Mean	Stdev
Band 1	3	3	3.000000	0.000000

Table(4) class distribution summary

Class Confusion Matrix

File

Confusion Matrix: F:\.results new\26april 2015results\New folder\CLUMP

Overall Accuracy = (2748/2764) 99.4211%
Kappa Coefficient = 0.9907

Ground Truth (Pixels)

Class	SOIL	VEG	WATER	Total
Unclassified	0	0	0	0
SOIL [Red] 12	1200	0	12	1212
VEG [Green] 1	4	1096	0	1100
WATER [Blue]	0	0	452	452
Total	1204	1096	464	2764

Ground Truth (Percent)

Class	SOIL	VEG	WATER	Total
Unclassified	0.00	0.00	0.00	0.00
SOIL [Red] 12	99.67	0.00	2.59	43.85
VEG [Green] 1	0.33	100.00	0.00	39.80
WATER [Blue]	0.00	0.00	97.41	16.35
Total	100.00	100.00	100.00	100.00

Class	Commission (Percent)	Omission (Percent)	Commission (Pixels)	Omission (Pixels)
SOIL [Red] 12	0.99	0.33	12/1212	4/1204
VEG [Green] 1	0.36	0.00	4/1100	0/1096
WATER [Blue]	0.00	2.59	0/452	12/464

Class	Prod. Acc. (Percent)	User Acc. (Percent)	Prod. Acc. (Pixels)	User Acc. (Pixels)
SOIL [Red] 12	99.67	99.01	1200/1204	1200/1212
VEG [Green] 1	100.00	99.64	1096/1096	1096/1100
WATER [Blue]	97.41	100.00	452/464	452/452

Table (5) Class Confusion matrix

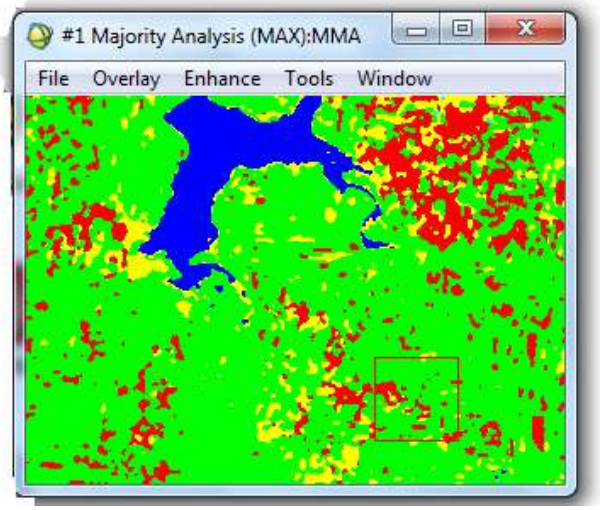

Fig (7). Classified Image (JUNE 15)

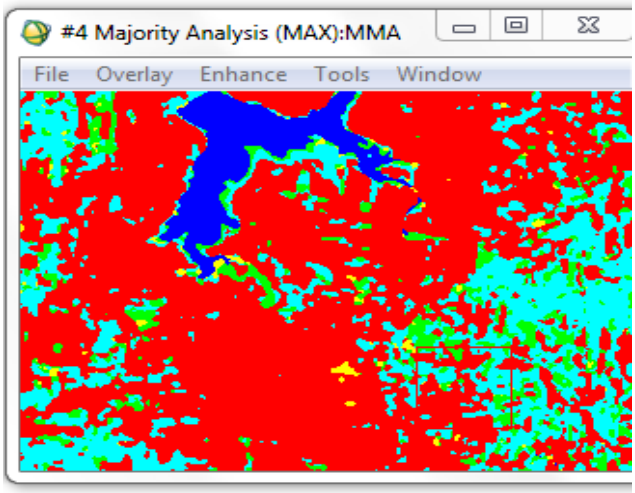

Fig (8). Classified Image (SEPT 20)

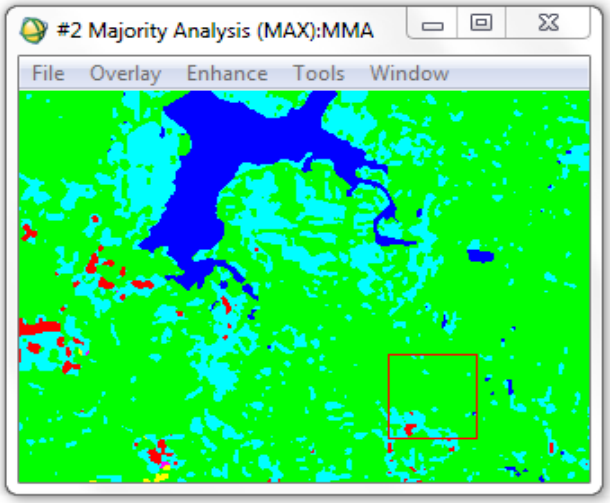

Fig (8). Classified Image (July 27)

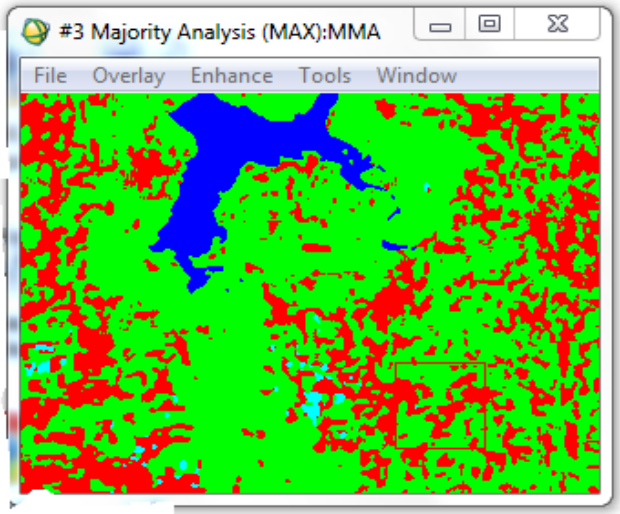

Fig (8). Classified Image (Aug 10)

Soil, Paddy, Water,
Sugarcane, Maize, Grass.

IV. DISCUSSION

The proposed algorithm is effectively boost the overall accuracy of crop type classification with synthetic or real data, we found that it will helpful for the formers and market management people who are balancing the market.

When the classifier used the small improvement occurred when high resolution images chosen for time to time of the year when the crop reflection curves are differed in most.

V. CONCLUSION

The goal of our work is to improve the crop type classification methods and help to the formers for getting the good value for their food grains, and also prove the increased efficiency by combining low and high resolution images for the identification and classification of crop types. Accurate and detailed crop type maps are very important for many reasons, and it is an ongoing work of the remote sensing community to develop the varies techniques for producing the crop maps.

REFERENCES

[1]. Mark W. Liu, Mutlu Ozdogan, and Xiaojin Zhu, "Crop Type Classification by Simultaneous Use of Satellite Images of Different Resolutions" IEEE TRANSACTIONS ON GEOSCIENCE AND REMOTE SENSING, VOL. 52, NO. 6, JUNE 2014.

[2]. C. Boryan, Z. Yang, R. Mueller, and M. Craig, "Monitoring US agriculture: The US Department of Agriculture, National Agricultural Statistics Service, Cropland Data Layer Program," *Geocarto Int.*, vol. 26, no. 5,pp. 341–358, 2011.

[3]. P. S. Thenkabail, C. M. Biradar, P. Noojipady, V. Dheeravath, Y. J. Li, M. Velpuri, M. Gumma, G. P. O. Reddy, H. Turral, X. L. Cai, J. Vithanage, M. Schull, and R. Dutta, "Global irrigated area map (GIAM), derived from remote sensing, for the end of the last millennium," *Int. J.Remote Sens.*, vol. 30, no. 14, pp. 3679–3733, 2009.

[4]. N. Guindin-Garcia, A. A. Gitelson, T. J. Arkebauer, J. Shanahan, and A.Weiss, "An evaluation ofMODIS 8- and 16-day composite products for monitoring maize green leaf area index," *Agricultural Forest Meteorol.*,vol. 161, pp. 15–25, Aug. 2012.

[5]. B.F. Wu and Q.Z. Li, "Crop planting and type proportion method for crop acreage estimation of complex agricultural landscapes," International Journal of Applied Earth Observation and Geoinformation, vol. 16, pp. 101-112, February 2012.

[6]. M.D. Nellis, K.P. Price, and D. Rundquist, "Remote sensing of cropland agriculture," The SAGE Handbook of Remote Sensing in 2009, SAGE Publications, April 2010.

[7]. H. North, D. Painnan, S. E. Belliss and J. Cuff, "Classifying Agricultural Land Uses with Time Series of Satellite Images," Int. Geosci. Remote Sens. Symp. (IGARSS '20J2), pp.5693-5696. 20 12.

[8]. K. L. Castro-Esau, G. A. Nchez-Azofeifa, B. S. Joseph-Wright, and M. Quesada, "Variability in leaf optical properties of Mesoamerican trees and the potential for species classification," *Amer. J. Botany*, vol. 93, pp. 517–530, 2006.